5th Workshop on Hyperspectral Image and Signal Processing: Evolution in Remote Sensing, WHISPERS 2013.
25-28 June 2013, Gainesville, Florida, USA.

CALIBRATION AND VALIDATION OF HYPERSPECTRAL IMAGERY USING A PERMANENT TEST FIELD

Lauri Markelin[1], Eija Honkavaara[1], Tuure Takala[2], Petri Pellikka[2]

[1]Finnish Geodetic Institute, P.O. Box 15, FI-02431 Masala, Finland (lauri.markelin, eija.honkavaara)@fgi.fi [2]Department of Geosciences and Geography, University of Helsinki, PO Box 64, 00014, Finland (tuure.takala, petri.pellikka)@helsinki.fi

ABSTRACT

Prerequisites for quantitative utilization of hyperspectral imagery are a physically based radiometric correction and accurate sensor calibration. An operational approach for calibration and validation (Cal/Val) would be the use of permanent test sites, which do not require campaign based reference measurements. In this article we present the Cal/Val results of the airborne hyperspectral imagery collected with AisaEAGLE-II sensor over the permanent Metsähovi remote sensing test field in Finland. Images were radiometrically corrected and reflectance accuracy of images based on both the laboratory and vicarious calibration was evaluated. The accuracy evaluation was based on the reference target reflectance in exact imaging geometry. Laboratory BRDF retrieved reflectance values were scaled with field nadir reflectance measurements acquired during the campaign to match with the imaging conditions. The transferability of the vicarious calibration performed over the Metsähovi was tested with the data taken in a different area a week later. The results indicated that the vicarious calibration improved the results in all evaluated cases.

Index Terms— test field, calibration, validation, hyperspectral, radiometric correction

1. INTRODUCTION

Hyperspectral imaging is increasingly used in various environmental remote sensing applications. Airborne hyperspectral sensors enable ground sampling distances (GSD) below 1 meter with high spectral resolution. In order to utilize this data quantitatively, an accurate radiometric correction of the imagery has to be performed. Several powerful correction approaches based on radiative transfer modeling are available for hyperspectral sensors [4, 9]. However, results of these methods have not been fully satisfying in all cases, thus block based approaches are being developed [1] and in the case of poorly calibrated sensors, mission based vicarious calibration is required [2]. In physically based correction methods, accurate sensor calibration is crucial. In this article we perform calibration and validation for airborne hyperspectral imagery collected with AisaEAGLE-II sensor. The process consists of the vicarious calibration of the sensor using the reference reflectance targets at the Metsähovi remote sensing test field [5, 6], the radiometric correction of the images and reflectance accuracy evaluation of the imagery. The accurate and cost-efficient vicarious calibration method based on permanent test fields would be a valuable tool for operators of hyperspectral imaging systems and of great importance for operational applications with hyperspectral images. This is, because of the fact that in operational applications the use of in-situ reference targets with in-situ reference measurements is not typically possible. The most cost-efficient approach would be to calibrate the sensor once or a few times during the imaging season.

2. MATERIALS AND METHODS

2.1. Imagery

The imagery was collected using AisaEAGLE-II hyperspectral sensor manufactured by the Specim Ltd. (www.specim.fi). The sensor works in VIS-NIR spectral range (400-1000 nm) with 1024 pixel swath width. The sensor was operated in 8x binning mode resulting in 64 channels with average width of 9.2 nm. The field of view (FOV) of the sensor is 37.7°.

We used imagery from two campaigns that were flown in summer 2011; first, over the Metsähovi test field of the Finnish Geodetic Institute (FGI) [60°15'N, 24°23'E], second, in the Porvoo agricultural test field [60°24'N, 25°37'E]. Two flight lines from Metsähovi (Msh) and one from Porvoo (Por) were used in this study (Table 1). The flying height was on average 500 meters above ground level resulting to a ground sampling distance (GSD) of 0.33 m in scan direction; in flight direction varying flight speed resulted to GSD of 0.3-0.4 m. Imagery was processed to constant GSD of 0.4 m. During the data processing there were some problems with the sensor spectral calibration which may add some uncertainty to results. The reference targets were located in the centre of the image line for Metsähovi Msh2 and at the border of the image line for Msh1 and Por4 lines.

Line	Date	Time [UTC+3]	F.h. [km]	F. Dir.	Sen Zen.	Sun Alt.	Sun Az.
Msh1	20.7.	13:03	0.53	90°	13.0°	50.2°	170.3°
Msh2	20.7.	13:16	0.56	180°	2.3°	50.4°	175.1°
Por4	27.7.	14:28	0.64	330°	15.7°	47.2°	202.5°

Table 1. Images used in this study. F.h. = flying height, F.Dir. = flying direction, SenZen. = average sensor zenith angle for the reference targets, SunAlt. & Az. = sun altitude and azimuth angles.

2.2. Reference measurements

Seven artificial reference reflectance targets were available at the Metsähovi test field (Figure 1): permanent black (B2a, B2b), gray (G2), white (W2) and red (R1) gravel targets, and two transportable painted tarpaulins (tarps P20, P30). In Porvoo, two portable tarps (P20, P30), gravel road, wheat field (Triticum aestivum) and oilseed rape field (Brassica napus subsp. oleifera) were used as reference targets (Figure 1).

Figure 1. Reference targets: Metsähovi (left) and Porvoo (right).

During the campaign the nadir reflectance spectra of the reference targets were measured using an ASD FieldSpec Pro FR spectrometer. The target reflectance was weighted with the AisaEAGLE-II channel spectral response to get the reflectance per channel. The accuracy of the averaged reflectance spectrum of the Metsähovi gravels and portable tarps is estimated to be well below 5%.

The reference target (Metsähovi gravels and portable tarps) anisotropic reflectance characteristics (BRDF retrieval) in exact imaging geometry for each image were measured in laboratory conditions using the FIGIFIGO goniospectrometer [10]. These laboratory measurements, scaled with the field nadir measurements, were used as a reference reflectance (ρ_{ref}) for the reflectance accuracy evaluation. The procedure is described in [7], and the reflectance properties of the targets in [6].

During both campaigns aerosol optical thickness (AOT) and water vapor column were measured using hand-held Microtops-II sunphotometer (Table 2). The atmospheric conditions were good during the Metsähovi campaign but more variable during the Porvoo campaign.

2.3. Radiometric correction

A total of three and two different reflectance image products were created from Metsähovi and Porvoo images respectively (Table 2), using ATCOR-4 software [8]. Options for sensor radiometric calibration were laboratory calibration by the sensor manufacturer (Lab) and vicarious in-flight calibration (Vic). Based on our earlier experiences and tests with ATCOR-4, atmospheric parameters were derived automatically from the image data using the ATCOR-4 modules (Table 2); also the variable visibility option was activated. The water vapor retrieval was based on the 820 nm absorption region. The more common 940 nm region was not used because of the used binning and low signal-to-noise-ratio (SNR) of the sensor channels above 900 nm. Two different vicarious calibrations were performed for Metsähovi images: image wise calibration based on reference targets B2a and W2 (Vic1), and one for the Msh2 image based on the reference targets B2a, G2, P30 and W2 (Vic2). Vic2 calibration was used for Msh1 and Por4 images to test the transferability of the calibration to different flight line and different areas. Outputs of these ATCOR-4 processing were radiometrically corrected reflectance image products.

	Image line	Msh1			Msh2			Por4	
	Version	Lab	Vic1	Vic2	Lab	Vic1	Vic2	Lab	Vic2
ATCOR	Vis. [km]	42.3	36.8	40.8	45.6	38.1	43.9	54.0	49.5
	AOT 550nm	0.205	0.230	0.213	0.185	0.214	0.191	0.166	0.178
	H_2O 820nm	1.78	1.39	1.21	2.47	1.64	1.61	3.84	2.81
In-situ	AOT 550nm	0.122			0.142			0.261	
	H_2O [g/cm^2]	1.62			1.64			2.59	

Table 2. Atmospheric parameters derived automatically from imagery by ATCOR-4 and measured in-situ.

2.4. Accuracy evaluation

The reflectance accuracy of the imagery was evaluated by calculating the absolute difference ($\Delta\rho$) of the measured image reflectance (ρ_{data}) and the reference reflectance (ρ_{ref}) in reflectance units: $\Delta\rho = \rho_{data} - \rho_{ref}$. Next this difference was divided by the ρ_{ref} and multiplied by 100 to get the relative reflectance difference $\Delta\rho$% in percents. $\Delta\rho$ and $\Delta\rho$% were calculated for all reference targets, image versions and sensor channels. From these differences, root mean square difference values (RMS and RMS%) were calculated using all reference targets (except targets used in calibration) for each image [7].

The sensor SNR was estimated from the imagery by calculating the ratio of reference target P30 average image reflectance to the standard deviation.

3. RESULTS

The results are shown mainly for Msh1 and Por4 images, as these lines presented the most demanding situation for the calibration and validation because of the largest of-nadir viewing angles and time and/or location difference compared to the Msh2 line. The SNR estimated from the Vic2 versions of each image line are shown in Figure 2. The SNR was highest on the 450-825 nm wavelength region. Due to the detected lower SNR of the channels above 900 nm, in the following only results with channels 1-54 are shown. The H_2O values derived automatically from the imagery were comparable to the in-situ measurements, but there were large differences with the AOT values.

3.1. Calibration

The sensor calibration parameters for adjusting the sensor laboratory calibration based image DNs to radiance are shown in Figure 2. The vicarious calibration compensated some disturbances in the 450-550 nm and 750-850 nm regions and corrected some general trends in both cal gain and offset parameters. The calibrations Vic1 and Vic2 based on the same image Msh2 were quite similar to each other while the version Msh1-Vic1 was more different from others especially in offset parameter.

3.2. Reflectance accuracy

The reference target reflectance spectra measured from the Lab and Vic2 versions of the Msh1 and Por4 image lines are shown in Figure 4. When laboratory calibration was used there were some visible disturbances (fluctuation) in the reflectance spectra, especially with the W2, P20 and P30. The use of vicarious calibration compensated for these disturbances.

Example of the absolute reflectance differences are shown in Figure 3. The maximum difference for Msh Lab versions was 0.04 for W2, -0.02 for P20 and P30, and 0.03 for other gravels. The vicarious calibration improved the accuracy especially for target W2, and for gravels B2a, B2b and G2 in the channels above 750 nm. The relative reflectance difference for Msh lab versions was between ±10% for all targets in the 400-600 nm range and for tarps, R1 and W2 also above 600 nm; for dark gravels the relative difference raised to level of 40% at 900 nm. After the vicarious calibration, the relative difference was below 10% for all targets.

For Porvoo Lab version, the reflectance difference was between ±0.03 for tarps and gravel, between ±0.01 for wheat and ±0.04 for rape. The accuracies improved slightly especially for tarps with the Vic2 version using vicarious calibration from the Metsähovi. In relative terms, the differences were between ±10% for all targets except rape. The red-edge around 700 nm caused the largest errors for the rape, which indicated some problems with the sensor spectral calibration.

The RMS plots in percents for all evaluated image versions are shown in Figure 4, right. The effect of the vicarious calibration can be seen in the channels above 750 nm, where the RMS% raised for the both Msh Lab versions, but vicarious calibration eliminated these drifts. With the vicarious calibration, reflectance accuracy level of 5% was achievable. The RMS in reflectance units varied between 0.005 and 0.022, and was in general lowest for Msh2-Vic1 and highest for Msh2-Lab versions.

The vicarious calibration Vic2 that was based on the image Msh2 performed well with the Msh1 image giving results comparable to image line-based Vic1 calibration. For Porvoo image, the Metsähovi Vic2 calibration slightly improved the reflectance accuracy when compared to the Por4 Lab version. In general, the laboratory calibration performed better with the Porvoo image than with the Metsähovi images, especially at the channels above 750nm.

4. SUMMARY AND DISCUSSION

The achieved absolute reflectance difference with vicarious calibration was between ±0.02 in reflectance units even for bright targets, which indicates higher accuracy compared to the results of Richter and Schläpfer [8] and comparable to results acquired with multispectral photogrammetric sensors [7].

One of our objectives was to improve the calibration and validation process by taking into account the reflectance anisotropy. The calibration of the AISA is carried out in the laboratory of Specim while the reference reflectance measurements in field and in the laboratory are based on

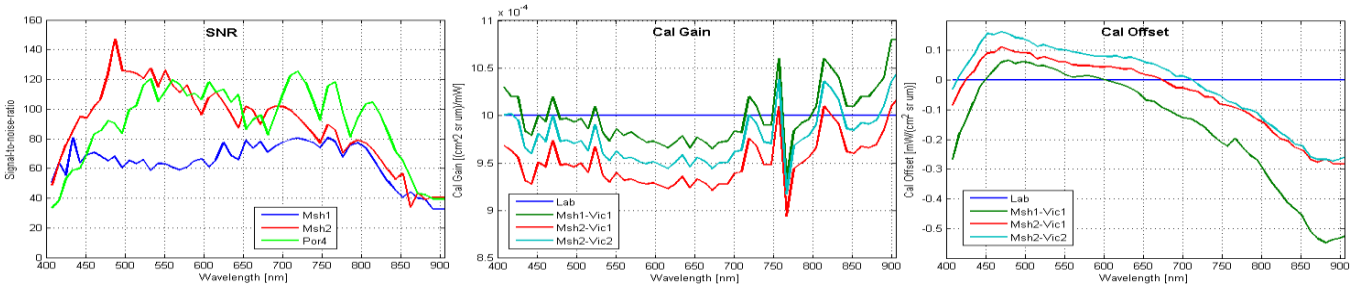

Figure 2. Left: sensor SNR estimated from three images; Gain (middle) and Offset (right) radiometric calibration parameters for each calibration version used.

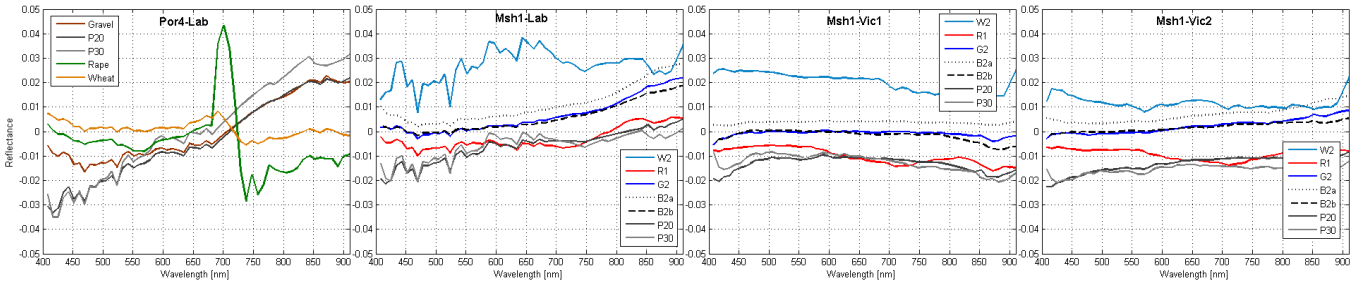

Figure 3. Reference target absolute reflectance difference for Por4-Lab and all versions of Msh1 image line.

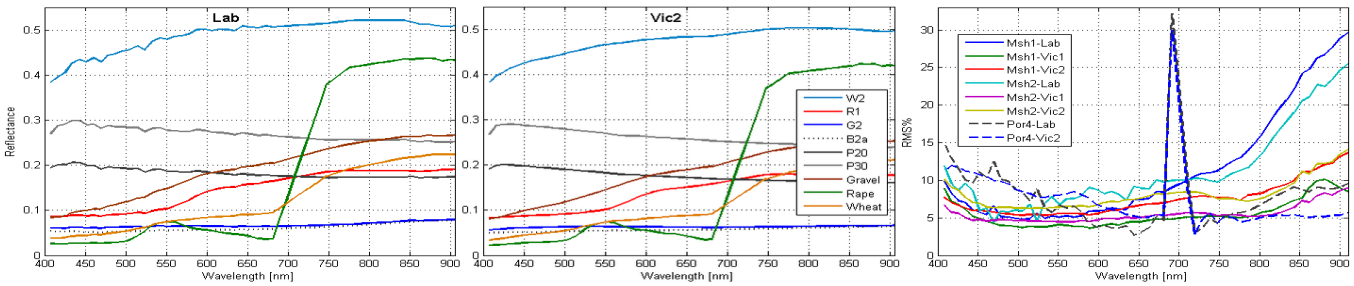

Figure 4. Reference target reflectance spectra for Lab (left) and Vic2 (middle) image versions. Gravel, rape and wheat are from Por4, others from Msh1. The spectra of B2a and B2b were practically identical. Right: reflectance RMS in percents; all evaluated image versions.

FGI's Spectralon panel and ASD spectrometer. At the moment the uncertainty and SI traceability [3] of both of these processes is unknown for us. The differences of the image based reflectance and the reference reflectance can be partially due to this traceability gap in the measurement chain. We will take this into account more rigorously in our further studies. However, the evaluation indicated that the tested vicarious calibration methods were advantageous because they compensated for the artifacts in the object spectrums.

Our experiences have shown that in operational calibration and validation procedures, permanent test fields are highly recommendable [5, 6, 7]. Networks of permanent test sites are under development for satellite systems [3], and national permanent test sites would be needed for airborne sensors. In difficult climate conditions, like in Finland, in addition to high quality reference targets also automatic in-situ reflectance measurement systems are needed. Our measurement arrangements could be considered as a prototype of such a system. The presented methodology provides new scientific information in comparison to other recent studies with hyperspectral systems by using weather resistant permanent reference targets, combining reference target anisotropy characterization in laboratory to in-situ reflectance measurements and by considering necessary in-situ atmospheric reference measurements.

5. REFERENCES

[1] Asmat, A., Milton, E.J., Atkinson, P.M., 2011. Empirical correction of multiple flightline hyperspectral aerial image mosaics. *Remote Sensing of Environment* 115, pp.2664-2673.

[2] Brook, A., Ben-Dor, E., 2011. Supervised vicarious calibration (SVC) of hyperspectral remote-sensing data. *Remote Sensing of Environment* 115, pp. 1543-1555

[3] Chander,G., Hewison, T., Fox, N., Wu, X., Xiong, X., Blackwell. W., 2013. Overview of intercalibration of satellite instruments. *IEEE Transactions in Geoscience and Remote Sensing*, 25 pages, doi:10.1109/TGRS.2012.2228654

[4] Gao, B.-C., Montes, M., Davis, C., Goetz, A., 2009. Atmospheric correction algorithms for hyperspectral remote sensing data of land and ocean. *Remote Sensing of Environment* 113, pp. 17-24.

[5] Honkavaara, E., Peltoniemi, J., Ahokas, E., Kuittinen, R., Hyyppä, J., Jaakkola, J., Kaartinen, H., Markelin, L., Nurminen, K., Suomalainen, J., 2008. A permanent test field for digital photogrammetric systems. *Photogrammetric Engineering & Remote Sensing* 74, pp. 95-106.

[6] Honkavaara, E., Hakala, T., Peltoniemi, J., Suomalainen, J., Ahokas, E., Markelin L., 2010. Analysis of Properties of Reflectance Reference Targets for Permanent Radiometric Test Sites of High Resolution Airborne Imaging Systems. *Remote Sensing*, 2(8): 1892-1917.

[7] Markelin, L., Honkavaara, E., Schläpfer, D., Bovet, S., Korpela, I., 2012. Assessment of radiometric correction methods for ADS40 imagery. *Photogrammetrie, Fernerkundung, Geoinformation (PFG)* 2012 (3), pp. 0251-0266.

[8] Richter, R., Schläpfer, D., 2002: Geo-atmospheric processing of airborne imaging spectrometry data. Part 2: atmospheric / topographic correction. *International Journal of Remote Sensing* 23 (13), pp. 2361–2649.

[9] Secker, J., Staenz, K., Gauthier, P., Budkewitsch, P., 2001. Vicarious calibration of airborne hyperspectral sensors in operational environments. *Remote Sensing of Environment* 76, pp. 81-92.

[10] Suomalainen, J., Hakala, T., Peltoniemi, J., Puttonen, E., 2009. Polarised multiangular reflectance measurements using the Finnish geodetic institute field goniospectrometer. *Sensors*, 9(5): 3891-3907.